Reliable Temperature Measurement in Radiation-Intensive Environments

Pablo Petrashin
Universidad Católica de Córdoba
Córdoba, Argentina
pablo.petrashin@ucc.edu.ar

Walter Lancioni
Universidad Católica de Córdoba
Córdoba, Argentina
walter.lancioni@gmail.com

Agustín Laprovitta
Universidad Católica de Córdoba
Córdoba, Argentina
alaprovitta@ucc.edu.ar

Juan Castagnola
Universidad Católica de Córdoba
Córdoba, Argentina
juancastagnola@ucc.edu.ar

***Abstract*— Radiation-resistant temperature sensors are vital for ensuring reliability in radiation-intensive environments, where the highly energetic and penetrating nature of radiation can significantly impact electronic devices and sensors. In such environments, like those near intense radiation sources or in challenging radiation-rich settings, such as space, gamma radiation can lead to erroneous measurements or equipment failures. Radiation-resistant sensors play a crucial role in maintaining measurement accuracy as they are designed to minimize interference caused by radiation, protecting electronic components and providing precise and reliable temperature readings. Their resilience to radiation-induced effects ensures data durability, reducing the need for frequent replacements, and enhancing the overall reliability of measurements in these demanding conditions. In this paper, we present and analyze two different configurations, aiming to address the challenges posed by radiation in sensitive environments. By exploring these novel approaches, we seek to enhance the robustness and accuracy of temperature sensors in radiation-intensive settings, enabling reliable data collection and facilitating successful operations in challenging radiation-rich conditions. The comparative analysis of these configurations will shed light on their performance and effectiveness in mitigating radiation-induced effects, thereby contributing to the advancement of radiation-resistant temperature sensing technologies.**

Keywords—highly linear, radiation-resistant, temperature sensors.

I. Introduction

In the context of electronic devices, such as transistors, exposure to radiation and temperature variations can significantly impact their performance, leading to challenges in circuit design for critical applications. Notably, the threshold voltage of pMOS (p-channel Metal-Oxide-Semiconductor) transistors becomes more negative with radiation, while nMOS (n-channel Metal-Oxide-Semiconductor) transistor threshold voltage, which is positive, decreases with temperature [1, 2-4]. This phenomenon is illustrated in Figure 1.

In contrast, when temperature varies, the negative threshold voltage of pMOS transistors becomes less negative, approaching zero, and the threshold voltage of nMOS transistors also approaches zero, becoming smaller [5- 9]. This behavior is depicted in Figure 2.

Taking advantage of the counter-phase behavior of these threshold voltage variations, a novel circuit design is presented to harness these effects for radiation compensation while simultaneously enabling temperature measurement.

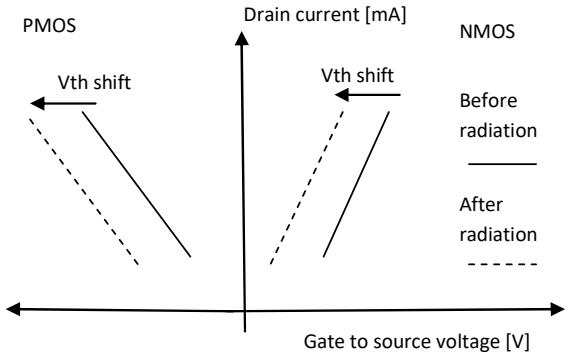

Fig. 1. Threshold voltage shift Vth due to the oxide trapped charges, after [1].

The circuit takes advantage of the radiation-induced shift in pMOS threshold voltage, which can be compensated with the same shift in nMOS threshold voltage.

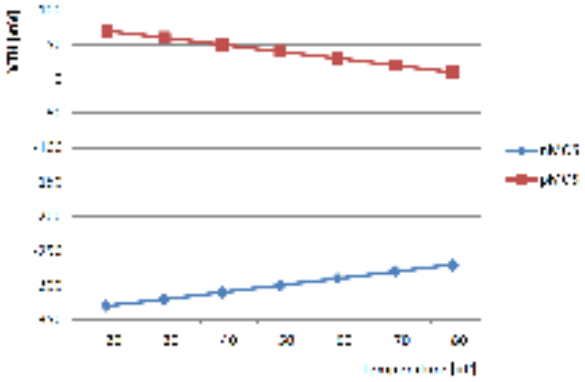

Fig. 2. Threshold voltage variation with temperature, after [4]

By carefully engineering this counteraction, the circuit achieves a robust compensation for the sensor's radiation sensitivity, while concurrently enabling accurate temperature measurement.

This novel idea represents a promising approach to mitigate the detrimental effects of radiation on electronic devices, particularly in harsh environments such as space

 How to cite: Petrashin, P., Lancioni, W., Laprovitta, A., Castagnola, J. (2024). Reliable Temperature Measurement in Radiation-Intensive Environments. *JAREE (Journal on Advanced Research in Electrical Engineering), 8(1).*

missions or nuclear applications. By capitalizing on the inherent behavior of pMOS and nMOS transistors with respect to radiation and temperature, the circuit demonstrates its potential to enhance the reliability and performance of integrated systems operating in challenging radiation-rich conditions. The detailed analysis of this circuit's efficacy will be presented in the subsequent sections, showcasing its significance in advancing radiation-hardened electronics and temperature sensing.

II. Proposed Configurations and Analysis

The proposed circuit introduces, in both approaches, a dual-branch configuration, as illustated in figure 3, where one branch is implemented by pMOS transistors (M1 and M2) and the other with nMOS transistors (M3 and M4). This innovative arrangement offers a strategic approach to nullify the mobility variation per branch, which is a critical parameter susceptible to changes caused by temperature and radiation effects. By effectively canceling out the mobility fluctuations, the circuit aims to achieve enhanced stability and precision in its output characteristics. Similar configuration was used for other purposes, such in [10].

For this preliminary analysis, the body effect of transistors M1 and M3 will be disregarded to simplify the initial assessment. The primary focus is on harnessing the counter-phase characteristics of pMOS and nMOS transistors concerning temperature and radiation-induced variations in their threshold voltages.

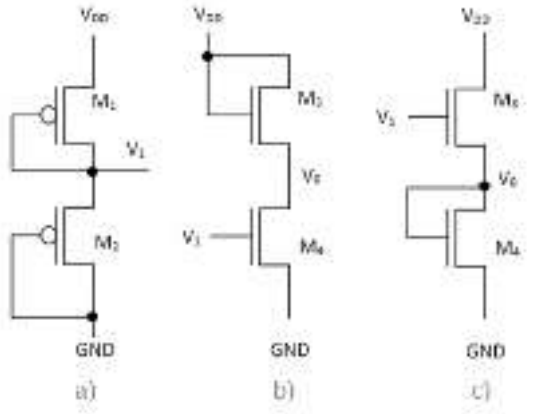

Fig. 3. Proposed configuration for the CMOS sensor: a) pMOS branch, b) First approach for nMOS branch, c) Second approach for nMOS branch

A. First approach

Figures 3a and 3b illustrate the distinct branches of the proposed circuit, showcasing the respective arrangement of pMOS and nMOS transistors. The circuit's design capitalizes on the inherent behavioral differences between the two transistor types, leveraging their individual responses to temperature and radiation conditions.

This strategic implementation allows for the potential compensation of radiation-induced effects on both branches and enhance the temperature-induced effects, thereby enabling accurate and reliable measurements in challenging radiation-rich environments [11-16].

Further research and experimental analyses will be carried out to validate the circuit's performance and potential advantages in mitigating the impact of radiation on electronic devices. The subsequent sections will go deeper into the detailed exploration of this novel proposal and its applicability in various radiation-sensitive applications.

Applying circuital analysis proposed in [17]:

For the pMOS branch, it can be derived the following:

$$V_1=\beta_2((V_{DD}-V_{TP})+V_{TP})(1+\beta_2) \quad (1)$$

In a similar way as done for obtaining (1), the branch shown in 3b is analyzed, giving the following result for the whole circuit with branches 3a and 3b:

$$Vo = V_{DD}\,(1- \beta_1\,\beta_2/(1+\beta_2)) + V_{TN}\,(\beta_1 - 1) + V_{TP}\,(\beta_2 - 1)\,\beta_1 / (1+\beta_2) \quad (2)$$

Where:

$$\beta_1= ((W/L)_4/(W/L)_3)^{1/2} \text{ and } \beta_2= (W/L)_1/(W/L)_2)^{1/2}$$

As it can be seen from eq. (2), Vo has three terms, one depending on V_{DD}, and the others related to V_{TN} and V_{TP}.

We need the coefficients of V_{TN} and V_{TP} variations to have opposite signs and equal magnitudes. Let's analyze the equation and find the relationship between β_1 and β_2 to achieve this:

Cancellation of V_{TN} and V_{TP} variations with respect to radiation:

To achieve cancellation, we require that the coefficients of V_{TN} and V_{TP} variations with respect to radiation have opposite signs and equal magnitudes. In other words, we need:

$$V_{TN}(\beta_1 - 1) = -V_{TP}(\beta_2 - 1)\beta_1/(1 + \beta_2) \quad (3)$$

Let's consider that the variations of VTN and VTP with respect to radiation can be represented by a parameter "k" as follows:

$$V_{TN} = k\,|V_{TP}| \quad (4)$$

Substitute this into the previous equation:

$$kV_{TP}\,(\beta_1 - 1) = -V_{TP}(\beta_2 - 1)\beta_1/(1 + \beta_2) \quad (5)$$

Now, cancel out the common factor of V_{TP}:

$$k(\beta_1 - 1) = -(\beta_2 - 1)\beta_1/(1 + \beta_2) \quad (6)$$

Rearrange the equation to isolate β1:

$$\beta_1 = (-(\beta_2 - 1)\beta_1/(1 + \beta_2))/k + 1 \quad (7)$$

By carefully selecting the values of β_2 and k based on the relative difference between V_{TN} and V_{TP} variations with respect to radiation, designers can ensure the desired radiation cancellation effect for Vo, even when the variations of V_{TN} and V_{TP} are not equal. This relationship between β_1 and β_2 will allow for a stable Vo in radiation-rich environments without introducing additional parameters.

In figure 4, it is shown Vo as a function of β2, with some fixed parameters: k=2.3, V_{DD}=3V, V_{TN}= 0.8V, $|V_{TP}|$=0.35V. Figure 4 can be used for positioning Vo at a desired value before reading the temperature.

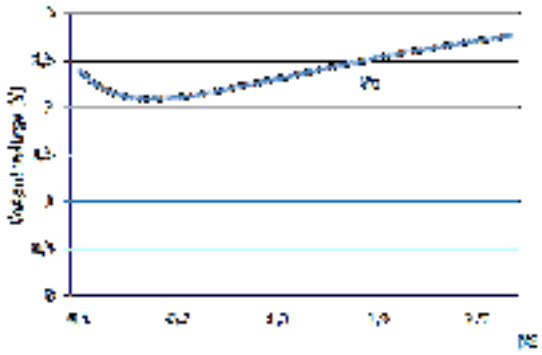

Fig. 4. Output voltage as a function of β2 for the first proposal

Once β2 and hence Vo are fixed, the circuit, to a first order approach, the circuit will react only with temperature, as shown in figure 5.

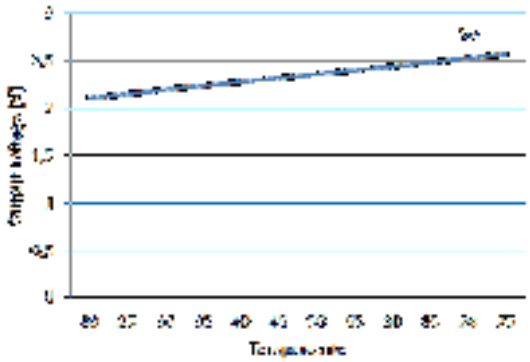

Fig. 5. Output voltage as a function of Temperature for eq. (2).

As it can be seen, the output voltage is highly linear for temperature dependency.

B. Second approach

Figures 3a and 3c illustrate the two branches of the proposed circuit for this second version analyzed. Again the circuit's design capitalizes on the inherent behavioral differences between the two transistor types, leveraging their individual responses to temperature and radiation conditions.

Using similar procedure as in previous case, Vo can be derived as follows:

$$Vo = V_{DD}\ \beta_2/((1 + \beta_2)(1 + \beta_1)) + V_{TN}(\beta_1 - 1)/ (1 + \beta_1) + V_{TP}(1 - \beta_2)/((1+\beta_1)(1 + \beta_2)) \quad (8)$$

Same as before, to achieve the cancellation of V_{TN} and V_{TP} variations with respect to radiation it is needed the coefficients of V_{TN} and V_{TP} variations to have opposite signs and equal magnitudes. In other words:

$$V_{TN}(\beta_1 - 1)/ (1 + \beta_1) = -V_{TP}(1 - \beta_2)/((1+\beta_1)(1 + \beta_2)) \quad (9)$$

Without introducing additional parameters, we can rewrite the condition for cancellation:

$$V_{TN}(\beta_1 - 1)/ (1 + \beta_1) = V_{TP}(\beta_2 - 1)/((1+\beta_1)(1 + \beta_2)) \quad (10)$$

To achieve the cancellation of VTN and VTP variations with respect to radiation, β1 and β2 should satisfy the above equation. As in previous paragraph, same as before, if it is considered that the variations of VTN and VTP with respect to radiation can be represented by a parameter "k" it follows:

$$V_{TN} = k|V_{TP}|$$

Substituting this into the previous equation and rearranging we can rewrite the final equation for Vo as follows:

$$Vo = V_{DD}\ \beta_2/((1 + \beta_2)(1 + ((1 - \beta_2)/k + 1))) + V_{TN}(((1 - \beta_2)/k + 1) - 1)/ (1 + ((1 - \beta_2)/k + 1)) + V_{TP}(1 - \beta_2)/((1 + ((1 - \beta_2)/k + 1))(1 + \beta_2)) \quad (11)$$

A graph of this equation is shown in figure 6, same as before, Vo as a function of β_2.

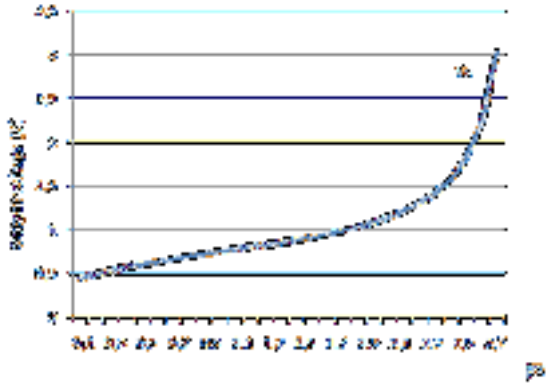

Fig. 6. Output voltage as a function of β_2 for the second proposal

As it can be seen, comparing figures 4 and 6, Vo can be set in a wide range of values, depending on the application.

III. Discussion on both approaches

Comparison of eq. (2) and (8) leads to the following conclusions:

Form and Structure: Equation (2) and Equation (8) have distinct structural differences. Equation (2) incorporates multiplication of β_1 and β_2 terms, which is absent in Equation (8). The denominator terms also differ, reflecting the variations in their mathematical formulations.

Parameter Interaction: In Equation (2), the interaction between β_1 and β_2 is multiplicative, affecting the cancellation and magnification behavior. Equation (8), however, separates the effects of β_1 and β_2 into distinct terms, potentially allowing for more straightforward analysis of their individual impacts.

Transistor Relationships: Both equations involve V_{TN} and V_{TP} terms in relation to their respective β_1 values. However, Equation (8) introduces a division by $(1 + \beta_1)$, which can influence the behavior of V_{TN} and V_{TP} in a different manner compared to Equation (2).

Dependency on β_1 and β_2: In Equation (2), the interplay between β_1 and β_2 is more directly pronounced due to the

multiplication, whereas Equation (8) separates the roles of β_1 and β_2 in the denominator terms.

Ease of Interpretation: Equation (8) appears to have a more intuitive structure, with a clear delineation of the effects of β_1 and β_2. This could aid in understanding the individual contributions of these parameters to the overall output.

Sensitivity: The sensitivity of each equation to changes in β_1 and β_2 might differ due to their distinct mathematical expressions. Careful analysis is required to determine how variations in these parameters impact the resulting Vo.

A. Sensitivity to β_1:

Equation (2): Changes in β_1 affect both the $\beta_1\ \beta_2/(1 + \beta_2)$ and the $\beta_1 / (1+\beta_2)$ terms. An increase in β_1 would lead to a decrease in the former term and an increase in the latter term. Overall, changes in β_1 would have complex, non-linear effects on the equation value.

Equation (8): Changes in β_1 directly affect the $V_{TN}(\beta_1 - 1)/ (1 + \beta_1)$ term. An increase in β_1 would increase the equation value, with the sensitivity being more linear compared to Equation (2).

B. Sensitivity to β2:

Equation (2): Changes in β_2 influence the $\beta_1\ \beta_2/(1 + \beta_2)$ term as well as the $(1+\beta_2)$ denominator. Changes in β_2's add to the overall sensitivity.

Equation (8): Changes in β_2 directly impact the $V_{DD}\beta_2$ term, contributing to an increase in the equation value. The sensitivity to β_2 is more straightforward in Equation (2).

Equation (2) exhibits non-linear and intricate sensitivity to changes in both β_1 and β_2. The combined effects of these parameters on cancellation and magnification require careful balancing. Small variations in β_1 and β_2 can lead to significant changes in the equation value, demanding precise calibration.

By the other hand, equation (8) demonstrates more linear sensitivities to both β_1 and β_2. Changes in these parameters have relatively more straightforward impacts on the equation value. This linear response simplifies the analysis and potential parameter adjustments.

Parameter Interaction: The interaction between β_1 and β_2 is crucial in both equations. Achieving the desired cancellation and magnification effects necessitates a delicate interplay between these parameters. The sensitivity of each equation underscores the need for accurate parameter selection and calibration.

Practical Implementation: Understanding the sensitivities of the equations aids practical implementation. Engineers can use this knowledge to optimize the parameter values, ensuring the desired performance characteristics and accurate temperature measurements in radiation-resistant environments.

In summary, sensitivity analysis reveals that Equation (8) demonstrates more linear and straightforward responses to changes in β_1 and β_2, simplifying the design process. Equation (2)'s non-linear sensitivities require careful consideration and potentially more intricate adjustments. Designers should leverage this understanding to effectively harness the cancellation and magnification effects while ensuring reliable temperature sensing in radiation-intensive conditions.

From the point of view of mathematical approach, the sensitivity of eq. (2) and (8) with respect to β_1 and β_2 can be found as:

For equation (2):

Partial derivative with respect to β_1:

$$\partial Vo/\partial\beta_1 = -V_{DD}\ \beta_2 / (1 + \beta_2) + V_{TN} - V_{TP}\ (\beta_2 - 1) / (1 + \beta_2)^2 \quad (12)$$

Partial derivative with respect to β_2:

$$\partial Vo/\partial\beta_2 = -V_{DD}\ \beta_1 / (1 + \beta_2)^2 + V_{TP}\ \beta_1 / (1 + \beta_2)^2 + V_{TP}\ (\beta_2 - 1)\ \beta_1 / (1 + \beta_2)^2 \quad (13)$$

For equation (8):

Partial derivative with respect to β_1:

$$\partial Vo/\partial\beta_1 = -V_{DD}\ \beta_2 / ((1 + \beta_2)(1 + \beta_1)\text{^}2) + V_{TN} / (1 + \beta_1)^2 + V_{TP}(1 - \beta_2) / ((1 + \beta_1)^2(1 + \beta_2)) \quad (14)$$

Partial derivative with respect to β_2:

$$\partial Vo/\partial\beta_2 = V_{DD} / ((1 + \beta_2)^2(1 + \beta_1)) - V_{DD}\ \beta_2 / ((1 + \beta_2)^2\ (1 + \beta_1)) + V_{TP} / ((1 + \beta_2)^2(1 + \beta_1)) \quad (15)$$

Analysis of equations (12) trough (15) leads to the following conclusions:

The partial derivatives of Equation (2) with respect to β1 and β2 are both more complex and include terms that involve both β1 and β2. The derivative with respect to β1 includes terms that can either increase or decrease the value of Vo based on their sign. The derivative with respect to β2 similarly includes terms with varying impacts, which can complicate the analysis and optimization of the equation.

The partial derivatives of Equation (8) with respect to β1 and β2 have simpler forms compared to Equation (2). The derivatives are expressed in terms of fractions involving powers of (1 + β1) and (1 + β2), resulting in a more straightforward interpretation of their effects on Vo.

Given the complexity of the derivatives and the relative simplicity of Equation (8)'s derivatives, Equation (8) appears again to be more straightforward to work with in terms of sensitivity analysis and optimization. The clearer structure of its derivatives makes it easier to understand how changes in β1 and β2 will affect the output Vo. Therefore, from an analytical perspective, Equation (8) is likely a better choice for practical applications where a clear understanding of sensitivity to parameter variations is essential.

However, the choice between the two equations ultimately depends on the specific requirements and constraints of the application. Both equations have unique characteristics, and the decision should take into consideration factors such as the desired cancellation/magnification effects, linearity, and ease of implementation. Careful analysis and consideration of the specific context will guide the selection of the most suitable

equation for the given radiation-resistant temperature sensing application

IV. Measurements

If the integrated version is considered, any pair of values for β_1 and β_2 is possible but doing this is not possible in practice. To conduct practical tests without the need to fabricate the integrated circuit, researchers often employ commercially available integrated circuits that have been extensively investigated for various purposes, such as the CD4007 [18-20]. Due to the accessibility of this integrated circuit, tests have been conducted with some key values of β_1 and β_2. To implement a feasible testing circuit using CD4007, certain approximations are necessary, especially because only fixed W/L (width/length) ratios can be found inside this chip. Firstly, it is assumed that the temperature coefficients of both p and n transistors are equal in absolute value, which is quite accurate for this specific IC. Secondly, it is clear that not all W/L relationships are possible; due to the fact that all transistors of the same type are equal, only values proportional to 2^n are achievable. For calculations using equation (6), β_2 is adopted as 0.7 for this example, resulting in a relation of ½ between $(W/L)_1$ and $(W/L)_2$. Consequently, β_1 is determined as 1.2, indicating that $(W/L)_4/(W/L)_3 = 1.44$. Unfortunately, this precise value cannot be attained in this scenario, and the closest value achievable is 1.41, obtained by using two transistors in parallel to achieve $(W/L)_4/(W/L)_3 = 2$.

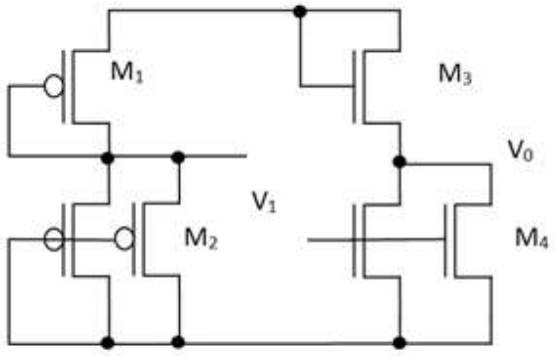

Fig. 7. Circuit implemented for measuring.

With these considerations the circuit that was simulated and then measured is illustrated in figure 7. As it can be seen, relations of 2 and ½ are achieved by putting in parallel two transistors of the same type. Each CD4007 has six transistors connected as inverters. Due to internal body potential connections, it resulted impossible to use only one chip for implementing the circuit with the proposed relations of 2 and ½. Two IC had to be used instead.

With the restrictions mentioned above, the circuit was built on an printed board and then submitted to a radiation source in order to validate the data used in previous section. The final board is shown in figure 8.

Fig. 8. A photograph of the testing circuit implementation using

After the irradiation procedure, the response of figure 9 has been achieved, coincident with [14, 17]. Applying constant biasing, ΔV_{TH0} increases in both P and N transistors. Given the fact that V_{TH0} variation is highly dependent on the biasing voltage, both P and N have been measured at constant biasing of ±9V respectively. The radiation dose was applied at a rate of 0.25 Gy/sec, for a total time of 120 seconds, giving an amount of 30 Gy.

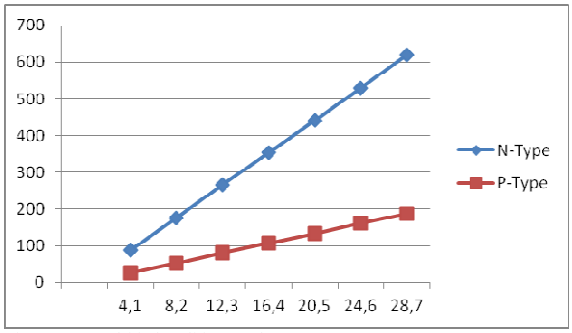

Fig. 9. V_{TH} shift for diferent doses.

V. Conclusions

The proposed temperature measurement configurations, as outlined in the preceding paragraphs, present distinct advantages over traditional methods in radiation-intensive environments. Utilizing a circuit with fewer than 10 transistors and constructed with standard CMOS technology, our approach not only streamlines complexity but also enhances cost-effectiveness. In contrast to thermocouples, RTDs, and thermistors, our configurations exhibit radiation independence, ensuring accurate temperature readings in the presence of gamma radiation. The linear output response across a broad temperature range underscores its reliability, surpassing the limitations of some existing technologies. Furthermore, the sensitivity analysis highlights the importance of precise calibration for optimal performance. While optical methods, such as pyrometer and fiber optic sensors, offer non-contact solutions, our configurations stand out for their simplicity, making them promising candidates for applications in space missions, nuclear facilities, and other critical systems where minimalistic design, robustness, and radiation resistance are paramount. The comparison with existing compensation techniques, as suggested by the reviewer, underscores the unique strengths and practical

significance of our proposed configurations in advancing temperature sensing technology for radiation-rich environments.

The significance of our study lies not only in the conceptual advancements of radiation-resistant temperature sensors but also in the robust quantitative results obtained through measurements, extensive simulations and analyses. The configurations presented in this research consistently exhibited remarkable radiation independence, highly linear temperature measurements, and resilient performance in radiation-rich environments. The non-linear sensitivity analysis of Equation (2) emphasizes the delicate balance required for parameter tuning, crucial for achieving the desired cancellation and magnification effects. Conversely, Equation (8) demonstrates a more straightforward response to parameter changes, simplifying the fine-tuning process. These quantitative insights not only reinforce the reliability and accuracy of our proposed configurations but also provide engineers with actionable data for optimizing sensor performance. The meticulous consideration of parameter interdependencies, as revealed by our sensitivity analyses, further supports the study's overarching goal of advancing radiation-resistant temperature sensing technology. In summary, our conclusion accentuates the quantitative foundation underpinning the proposed configurations, elucidating their practical implications and reaffirming their potential impact on critical systems and missions in radiation-intensive environments.

The analyzed configurations show promising results for achieving radiation-independent and highly linear temperature measurements. Its robustness and reliability make the proposal valuable candidate for applications in radiation-intensive environments, offering improved data accuracy and durability for critical systems and missions. The main features of this novel idea are:

Radiation-Independence: The configuration presented in this study shows its effectiveness in achieving temperature measurements independent of radiation. By minimizing the impact of gamma radiation on sensor performance, these configurations enhance the reliability and accuracy of temperature readings in radiation-intensive environments.

Linear Output: The circuit exhibit highly linear output response for temperature measurement. This linearity is crucial for obtaining accurate and consistent temperature data across a wide range of temperatures, making it a reliable solution for various applications.

Robust Performance: The simulations and analyses conducted on the configuration shows its robust performance in challenging radiation-rich settings. Its ability to maintain linear output and accurate temperature readings in the presence of radiation enhances its suitability for use in space missions, nuclear facilities, and other radiation-intensive applications.

Data Durability: The radiation-resistant nature of this sensor ensures data durability, reducing the need for frequent replacements. This attribute contributes to cost-effectiveness and long-term reliability in radiation-prone environments.

Promising Applications: The configurations' excellent linearity and radiation independence open up promising applications in scientific research, space exploration, nuclear power plants, and other critical systems where precise and reliable temperature measurements are essential.

When considering sensitivity analysis, equation (2) shows a non-linear sensitivity to changes in both β_1 and β_2. The interaction between these parameters, as evidenced by the multiplicative term $\beta_1 \beta_2/(1 + \beta_2)$, requires careful parameter balancing to achieve the desired cancellation and magnification effects. Small variations in β_1 and β_2 can lead to significant shifts in the equation value, highlighting the need for precise calibration and consideration of parameter interdependencies.

On the other hand, Equation (8) exhibits more linear sensitivities to β_1 and β_2. Changes in these parameters result in more straightforward adjustments to the equation value, simplifying the analysis and potential parameter selection. The linear response of Equation 2 facilitates a clearer understanding of how variations in β_1 and β_2 influence the overall system behavior, aiding engineers in fine-tuning the sensor's performance.

Both equations' sensitivity analyses emphasize the critical importance of selecting appropriate values for β_1 and β_2 to achieve the desired temperature measurement characteristics. Engineers must carefully consider the trade-offs between cancellation, magnification, and linearity, taking into account the specific requirements of the intended application and the challenges posed by radiation-rich environments.

Future Prospects: The study's findings provide valuable insights into the development of advanced radiation-resistant temperature sensors. Further research and refinement of this configuration could lead to even more efficient and versatile sensor designs for extreme radiation conditions.

REFERENCES

[1] Tatjana Pešić-Brđanin, “Spice Modelling of Ionizing radiation effects in CMOS Devices” FACTA UNIVERSITATIS Series: Electronics and Energetics Vol. 30, No 2, June 2017, pp. 161 - 178 DOI: 10.2298/FUEE1702161P

[2] Y. H. Lho, K. Y. Kim, “Radiation Effects on the Power MOSFET for Space Applications,” ETRI Journal, vol. 27, no. 4, Aug. 2005, pp. 449-452. DOI: 10.4218/etrij.05.0205.0031

[3] S. Golubovic, S. Dimitrijev, D. Zupac, M. Pejovic and N. Stojadinovic, "Gamma-Radiation Effects in CMOS Transistors," ESSDERC '87: 17th European Solid State Device Research Conference, Bologna, Italy, 1987, pp. 725-728.

[4] Nicolas Roisin, Thibault P. Delhaye, Nicolas André, Jean-Pierre Raskin, Denis Flandre, “Low-power silicon strain sensor based on CMOS current reference topology”, Sensors and Actuators A: Physical, Volume 339, 2022, 113491, ISSN 0924-4247.

[5] C. Viale, P. Petrashin, L. Toledo, W. Lancioni and C. Vazquez, “Single event effects in an analog SOI transconductor: a case study”, 2015 16th Latin-American Test Symposium (LATS), 25-27 March 2015, DOI: 10.1109/LATW.2015.7102408

[6] Felix Kunz, Pablo Petrashin, Gabriela Peretti, Eduardo Romero and Carlos Marqués, “Single-event Transients in OTA-C Analog Structures: A Case Study”. IETE, Journal of research. Volume 57, No 1, January-February 2011, ISSN 0377-2063

[7] S. H. Carbonetto, M. A. García-Inza, J. Lipovetzky, E. G. Redin, L. Sambuco Salomone, and A. Faigon, “Zero temperature coefficient bias in MOS devices. dependence on interface traps density, application to MOS dosimetry,” IEEE Trans. Nucl. Sci., vol. 58, no. 6, pp. 3348–3353, 2011.

[8] M. Soubra, J. Cygler, and G. Mackay, “Evaluation of a dual bias dual metal oxide-silicon semiconductor field effect transistor detector as radiation dosimeter,” Med. Phys., vol. 21, no. 4, pp. 567–572, 1994.

[9] J. R. Schwank, M. R. Shaneyfelt, D. M. Fleetwood, et al., "Radiation Effects in MOS Oxides," IEEE Trans. Nuclear Science, Vol. 55, no. 4, pp. 1833-1853, 2008.

[10] "Temperature compensated low voltage MOSFET radiation sensor: proof of concept and a case study" Pablo Petrashin, Walter Lancioni, Juan Castagnola, Agustín Laprovitta. ISSN: 2579-6216 - Journal on Advanced Research in Electrical Engineering, Dec. 2020

[11] "Embedded Radiation Sensor with OBIST Structure for Applications in Mixed Signal Systems". Pablo Petrashin, Walter Lancioni, Juan Castagnola, Agustín Laprovitta. ISSN: 2579-6216 - Journal on Advanced Research in Electrical Engineering, Vol 5, No 2, pp114-119, Sept.2021

[12] O. F. Siebel, M. C. Schneider and C. Galup-Montoro, "Low power and low voltage VT extractor circuit and MOSFET radiation dosimeter", 10th IEEE International NEWCAS Conference, 17-20 June 2012, DOI: 10.1109/NEWCAS.2012.6329016

[13] M.A. Carvajal, S. Garcia-Pareja, M. Vilches, D. Guirado, M. Anguiano, A.J. Palma, A.M. Lallena, "Simulated and experimental angular response of a commercial MOSFET used as dosimeter", Proceedings of the 2009 Spanish Conference on Electron Devices - Feb 11-13, 2009. Santiago de Compostela, Spain.

[14] O.F. Siebel, J.G. Pereira, M.C. Schneider, and C. Galup-Montoro, "A MOSFET dosimeter built on an off-the-shelf component for in vivo radiotherapy applications", 2014 IEEE 5th Latin American Symposium on Circuits and Systems 25-28 Feb. 2014, DOI: 10.1109/LASCAS.2014.6820261

[15] M. G. Buehler, B. R. Blaes, G. A. Soli, and G. R. Tardio, "ON-CHIP p-MOSFET DOSIMETRY", IEEE TRANSACTIONS ON NUCLEAR SCIENCE, VOL. 40, NO. 6, DECEMBER 1993

[16] Paul G. A. Jespers "A Simple graphical tool for MOS circuit analysis and design.", internal report at Université Catholique de Louvain La Neuve, Belgium

[17] O. F. Siebel, M. C. Schneider and C. Galup-Montoro, "Low power and low voltage VT extractor circuit and MOSFET radiation dosimeter", 10th IEEE International NEWCAS Conference, 17-20 June 2012, DOI: 10.1109/NEWCAS.2012.6329016